

# Clade-Specific Differences in Neurotoxicity of Human Immunodeficiency Virus-1 B and C Tat of Human Neurons: Significance of Dicysteine C30C31 Motif

Mamata Mishra, MPhil,<sup>1</sup> S. Vetrivel, MSc,<sup>1</sup> Nagadenahalli B. Siddappa, PhD,<sup>2</sup> Udaykumar Ranga, PhD,<sup>2</sup> and Pankaj Seth, PhD<sup>1</sup>

**Objective:** Human immunodeficiency virus-1 (HIV-1) causes mild to severe cognitive impairment and dementia. The transactivator viral protein, Tat, is implicated in neuronal death responsible for neurological deficits. Several clades of HIV-1 are unequally distributed globally, of which HIV-1 B and C together account for the majority of the viral infections. HIV-1-related neurological deficits appear to be most common in clade B, but not clade C prevalent areas. Whether clade-specific differences translate to varied neuropathogenesis is not known, and this uncertainty warrants an immediate investigation into neurotoxicity on human neurons of Tat derived from different viral clades.

**Methods:** We used human fetal central nervous system progenitor cell-derived astrocytes and neurons to investigate effects of B- and C-Tat on neuronal cell death, chemokine secretion, oxidative stress, and mitochondrial membrane depolarization by direct and indirect damage to human neurons. We used isogenic variants of Tat to gain insights into the role of the dicysteine motif (C30C31) for neurotoxic potential of Tat.

**Results:** Our results suggest clade-specific functional differences in Tat-induced apoptosis in primary human neurons. This study demonstrates that C-Tat is relatively less neurotoxic compared with B-Tat, probably as a result of alteration in the dicysteine motif within the neurotoxic region of B-Tat.

**Interpretation:** This study provides important insights into differential neurotoxic properties of B- and C-Tat, and offers a basis for distinct differences in degree of HIV-1-associated neurological deficits observed in patients in India. Additional studies with patient samples are necessary to validate these findings.

Ann Neurol 2008;63:366–376

The central nervous system (CNS) is susceptible to infection by retroviruses of various species, particularly the members of the lentivirus family.<sup>1</sup> According to the estimates of the World Health Organization, of more than 40 million human immunodeficiency virus (HIV)-infected individuals worldwide, the majority of cases and the greatest incidences of mortality are in developing countries such as South Africa, India, and China. HIV-1 directly affects the nervous system and causes distinct neurological deficits that involve loss of executive cortical functions and compromised cognitive and motor functions caused by significant neuronal death in the basal ganglia, cerebral cortex, and hippocampal regions. Nervous system infection with HIV-1 can produce a range of debilitating clinical disorders that manifest in the advanced stages of the viral infection.<sup>2</sup> The neurological deficits in HIV-1 patients

have been correlated to the amount of virion trafficking to the brain that is mostly dependent on the secretion of a chemoattractive cytokine, monocyte chemoattractant protein-1 (MCP-1; recently classified as CC chemokine ligand-2 [CCL2]) from the glial cells,<sup>3</sup> and to neuronal damage caused by the viral proteins. Chemokines such as MCP-1/CCL2 and CXCL-10/IP-10 are upregulated in HIV-1 patients with dementia as compared with HIV-1-positive individuals without dementia.<sup>4–6</sup> Levels of MCP-1/CCL2 correlate with cerebrospinal fluid viral load and the severity of dementia in HIV-1-infected individuals.<sup>4,7</sup> It has been demonstrated that HIV-1 enters the CNS at an early stage of infection breaching the blood-brain barrier. Macrophages and microglial cells are productively infected by the virus whereas astrocytes are nonproductively infected, and neurons are rarely infected.<sup>8</sup> As demon-

From the <sup>1</sup>National Brain Research Centre, Manesar (Gurgaon); and <sup>2</sup>Jawaharlal Nehru, Centre for Advanced Scientific Research, Bangalore, India.

Received May 31, 2007, and in revised form Aug 28. Accepted for publication Sep 28, 2007.

Published online Dec 11, 2007, in Wiley InterScience (www.interscience.wiley.com). DOI: 10.1002/ana.21292

Address correspondence to Dr Seth, Molecular and Cellular Neuroscience, National Brain Research Centre (NBRC), NH-8, Nainwal Mode, Manesar, Haryana-122050, India. E-mail: pseth@nbrc.res.in

strated by the pathological examination of postmortem brains, neurons constitute the cell type that is mostly affected by the viral infection. Up to 40% neuronal loss is accompanied with extensive damage to the dendritic arbor. Presence of HIV-1 particles within the neurons is, however, uncommon.<sup>9</sup> Infection of glial cells inflicts an excitotoxic and inflammatory response because there is an increase in glutamate levels and oxidative stress, together with overexpression of proinflammatory cytokines and chemokines, resulting in a neurotoxic environment for neurons. HIV-1-induced damage to neurons is via apoptosis, which is the main cause for HIV-1-associated dementia. Several viral and cellular factors contribute to the neuronal damage after HIV-1 invasion into the brain. Among the viral factors, viral proteins such as Tat, as well as the envelope protein, gp120, are neurotoxic. HIV-1 Tat has been detected in the brains of patients with HIV-1-associated dementia.<sup>10</sup> Tat, a small nonstructural transcriptional regulator, is crucial for the replication of HIV-1. Tat induces oxidative stress and causes neuronal death via activation of the intrinsic apoptotic pathway that involves disturbances in mitochondria, release of cytochrome *c*, calcium overload, and subsequently the activation of caspase cascade in neurons.<sup>11</sup> There is evidence to suggest that neurotoxic HIV-1 proteins released from cells harboring HIV-1 trigger oxidative stress in cell culture<sup>11</sup> and in animal models.<sup>12,13</sup>

The pandemic infection of HIV is attributed to its different clades (A–K) that are unequally distributed around the world as clusters in certain areas.<sup>14</sup> The research focus and majority of the clinical studies have been on HIV-1 clade B that is prevalent in North America and Europe, hence the biology of clade B is understood in greater detail. Some clade-specific differences in disease transmission, in the long terminal repeat region of HIV-1, and in viral replication have been reported previously.<sup>15–18</sup> However, it is currently unclear whether HIV-1 clades with different biological properties may cause differences in the progression of the disease pathogenesis, particularly in the human brain. In India, HIV-1 clade C accounts for more than 95% of HIV-1 infection.<sup>19</sup> Current epidemiological studies demonstrate that HIV-1 clade C is implicated in more than 50% of the cases of HIV infection worldwide,<sup>20</sup> and that env-based HIV-1 clade C would dominate an HIV-1 pandemic in the coming years.<sup>21</sup> HIV-1-associated dementia (HAD) is quite common in HIV-infected individuals with prevalence rates up to 40% in Western countries where clade B prevails. Contrary to the clinical picture observed in the West, the incidence of HIV-associated neurological complications in India is believed to be quite low, which may be because of a different HIV-1 clade C, although there are no experimental studies to prove this fact.<sup>22,23</sup> It is surprising that although HIV-1 clade C affects

more than half of the total HIV-infected individuals worldwide, there have been limited studies to understand the neurobiology of HIV-1 clade C and to explore the neurotoxic properties of its viral protein, Tat. Our search of the indexed medical journals showed lacunae in a number of studies that investigated the pathogenesis of HIV-1 clade C. At the genetic and molecular levels, HIV-1 clade C has been shown to differ from other subtypes in many ways; however, it is currently unknown whether these differences affect their pathogenic properties, particularly with reference to the CNS.<sup>24</sup> Because the knowledge available on HIV-1 clade C-associated HAD, as well as its neurobiology, is inadequate, there is an urgent need to conduct detailed studies on HIV-1 clade C. A previous study from some of us describing the structural and functional aspects of Tat from clades B and C provided experimental evidence that alteration in one of the differentially conserved amino acids in C-Tat decreased the chemotactic functions of Tat without affecting its transactivation properties.<sup>25</sup> The study also demonstrated high conservation of the CS motif at positions 30 and 31 of Tat among all the clade C strains regardless of their geographic distribution.

Using synthetic peptides spanning the entire sequence of Tat 1 through 86, earlier reports showed that a distinct, conformationally dependent region of Tat, within the first exon between positions 31 and 61, is responsible for most of its neurotoxic properties.<sup>26</sup> Hence it is quite likely that variations within the first exon of Tat, especially between positions 31 and 61, may alter the neurotoxic properties of the viral protein. However, a direct effect of the alteration seen at position 31 in Tat from clade B on neuronal damage or neurotoxicity and its consequence on neurodegeneration remains lacking in the literature to date.

This study aims to compare the neurotoxic properties of Tat derived from clades B or C. Primary neurons were either directly exposed to recombinant Tat proteins or to the conditioned media collected from human astrocytes transfected with expression vectors of HIV-1 clade B- or C-Tat. Using an array of assays including neuronal apoptosis, production of chemokine CCL2, levels of oxidative stress, and mitochondrial membrane depolarization, we found that C-Tat was significantly less neurotoxic than B-Tat. We believe that this study provides a basis for the observed low levels of HIV-1-associated dementia among a significantly large population of HIV-1-positive individuals in India, and perhaps other geographical regions where HIV-1 clade C is predominant.

## Subjects and Methods

### *Human Brain Cell Culture*

Human CNS cell cultures were prepared from 8- to 12-week-old embryos obtained from elective medical termina-

tion of first-trimester pregnancies performed at the local hospitals. The handling of fetal brain tissue was done after obtaining mother's consent, and samples were processed as per the protocols approved by the institutional human ethics committee in compliance with the recommendations of the Indian Council of Medical Research.

#### *Preparation of Cultures of Human Astrocytes and Neurons*

Primary cultures of human CNS progenitor cells were prepared and cultured as monolayers on poly-D-lysine-coated plastic ware in serum-free neurobasal media, and astrocytes and neurons were derived from them as described previously.<sup>27</sup> In brief, astrocyte differentiation was initiated by changing to Eagle's minimum essential medium supplemented with 10% fetal calf serum and 2mM glutamine; after 3 weeks, 99.9% of the cells were immunoreactive for astrocyte marker, glial fibrillary acidic protein (Dako, Carpinteria, CA). Neuronal differentiation involved changing the growth factors in the progenitor media to brain-derived neurotrophic factor (10ng/ml) and platelet-derived growth factor-A/B (10ng/ml) for 3 weeks. More than 98% of cells were positive for neuronal marker  $\beta$  III-tubulin (Covance, Berkeley, CA). All other reagents were purchased from Sigma Chemicals (St Louis, MO).

#### *Human Immunodeficiency Virus-1 Tat Expression Vectors and Tat Protein Preparation*

Construction of the wild-type subtype C-Tat mammalian-expression vector on the pcDNA3 vector backbone was described previously.<sup>25</sup> The wild-type C-Tat contains cysteine and serine residues at positions 30 and 31, respectively (CS). The CC and SC isogenic mutants of C-Tat were generated by means of site-directed mutagenesis using overlapping polymerase chain reaction as described elsewhere.<sup>25</sup> A mammalian expression vector of subtype B-Tat was also prepared from the HIV-1 molecular clone YU-2 (Cat #M2393, NIH AIDS Research and Reference Reagent Program) using a similar strategy. Human embryonic kidney 293 (HEK293) cells were transiently transfected with the pYU2 molecular clone, total cellular RNA was extracted after 72 hours, and complementary DNA was prepared in a reverse transcription reaction using the reverse primer N531 (5'-AGAAGC-GGATCCCTAATGGACCGGATCTGTCTCTGT-3'). The conditions for reverse transcription were incubation for 30 minutes at 42°C and 5 minutes at 94°C. The primer N531 in combination with the forward primer N113 (5'-TAGA-ATTCCGCCGCCATGGAGCCAGTAGATCCTAACC-TA-3') was used for polymerase chain reaction amplification. The amplification reaction mixture of 50 $\mu$ l contained 250nM of each primer, 100 $\mu$ M of each deoxynucleotide triphosphates, 1.25 units of *Taq* DNA polymerase, and 3.0mM MgCl<sub>2</sub>. Amplification was performed using the following cycling conditions, preamplification denaturation for 30 seconds at 94°C, followed by 35 cycles, with each cycle consisting of incubations at 94°C for 30 seconds, 60°C for 30 seconds, and 72°C for 30 seconds. The amplified product was purified using a column-based commercial kit (Qiagen, Hilden, Germany) and cloned directionally between *Eco*RI and *Eco*RV (destroyed) into a mammalian expression vector pcDNA 3.1+

(Invitrogen, Carlsbad, CA). Bacterial expression vectors encoding the wild-type B-Tat, C-Tat (CS), and the isogenic variants C-Tat (CC) and Tat (SC) were generated, and the recombinant proteins were purified as described previously.<sup>28</sup> Lyophilized pure Tat protein was dissolved in sterile endotoxin-free 1X phosphate-buffered saline (PBS) to prepare the stock solution of 1mg/ml and was stored as aliquots in presiliconized vials at -80°C for further use.

#### *Tat Treatment of Primary Human Astrocytes and Neurons*

Human astrocytes were plated at a density of  $2 \times 10^4$ /well in 24-cluster plates. After overnight culture, they were treated with up to 100ng/ml of recombinant Tat protein, incubated for an additional period of 24 hours, and the conditioned culture medium was collected. The collected media were assayed for CCL2 production and/or saved for subsequent treatment of neurons. Alternatively, the astrocytes were transfected with various Tat-expressing plasmid vectors or the control pcDNA3.1 plasmid using Lipofectamine reagent in OptiMEM media (Invitrogen, Carlsbad, CA) as per manufacturer's protocol. Conditioned media from transfected astrocytes were collected 24 hours later and centrifuged to remove any floating cells. Supernatants were used immediately to treat neurons or stored as aliquots at -80°C until further experimentation.

Human neurons were plated at a density of  $1 \times 10^4$  cells/well in chamber slides (Nunc, Roskilde, Denmark) in neuronal medium, cultured overnight, and exposed to HIV-1 B- and C-Tat protein at concentrations ranging from 10 to 100ng/ml for 24 hours by adding the protein directly to the neuronal cultures. Control cells received the vehicle, sterile 1X PBS. Alternatively, in parallel cultures of human neurons, half of the neuronal medium was replaced with conditioned medium obtained from astrocytes transfected with various Tat vectors.

#### *Measurement of Chemokine Monocyte Chemoattractant Protein-1/CC Chemokine Ligand-2 by Enzyme-Linked Immunosorbent Assay*

MCP-1/CCL2 chemokine protein levels were determined in astrocyte culture media collected after treatment with Tat protein or 24 hours after transfection with Tat vectors by enzyme-linked immunosorbent assay in cell-free supernatants, using the matched antibody pairs purchased from BD Biosciences (San Jose, CA) following manufacturer's protocol.

#### *Terminal Deoxynucleotidyltransferase-Mediated dUTP Nick End Labeling Assay*

After incubation of neurons for 24 hours with HIV-1 Tat by either of the methods described earlier, neurons undergoing apoptosis were identified by terminal deoxynucleotidyltransferase-mediated dUTP nick end labeling (TUNEL) assay using *In Situ* Cell Death Detection Kit, TMR red (Roche, Mannheim, Germany), as described earlier.<sup>29</sup> Images of TUNEL-positive cells and 4',6-diamidino-2-phenylindole (DAPI)-stained nuclei were taken from at least five random fields using a Zeiss Axioplan microscope (Carl Zeiss Company, Heidenheim, Germany) with charge-coupled device

camera. For TUNEL assay, a minimum of 100 neurons were measured from 3 to 5 different fields per condition. Using an image analysis system, we counted TUNEL-positive nuclei together with total DAPI-positive nuclei, and apoptosis was represented as percentage TUNEL-positive cells/DAPI.

#### *Cell Viability Assay or MTT Assay*

An MTT (3-[4,5-dimethylthiazol-2-yl]-2,5-diphenyl-tetrazolium bromide) assay was performed for assessing the neuronal cell viability. After incubation with HIV-1 Tat protein or conditioned media from astrocytes transfected with various Tat constructs for 24 hours, the MTT assay was performed on neuronal cells as per manufacturer's protocol. Viability of neurons was calculated by comparing with amount of formazan crystals formed. Vehicle controls or vector groups were taken as 100% viable, and test groups were compared with respective control samples.

#### *Neuronal Mitochondrial Membrane Assays*

After treatment with Tat protein or culture of neurons in neuronal media containing astrocyte conditioned media, neurons were incubated in JC-1 dye at a concentration of 1  $\mu$ g/ml. The fluorescence emission pattern of JC-1 was assessed 10 minutes after incubation using a fluorescent microscope (Zeiss, Heidenheim, Germany) in both red and green portions of the spectrum, and images of neurons were captured using a high-resolution with charge-coupled device camera.

For quantitation of JC-1 red and green aggregates, neurons were cultured and treated in parallel under similar conditions. Neurons were detached and JC-1 dye was added to cell suspension. Cell suspensions were then read at 525 and 590nm using a spectrophotometer (Lambda 40, UV/Vis Spectrophotometer; Perkin-Elmer, Waltham, MA), and ratios of red-to-green (590/525nm) optical density were calculated.

#### *Measurement of Reactive Oxygen Species*

To monitor the level of reactive oxygen species (ROS) produced within neurons subjected to Tat treatments or exposure to astrocyte media, we used the cell-permeable, nonpolar, H<sub>2</sub>O<sub>2</sub>-sensitive probe 5 (and 6)-chloromethyl-2', 7'-dichlorodihydrofluorescein diacetate (DCFDA), as described previously.<sup>30</sup> Control and treated neuronal cultures were incubated with DCFDA (5  $\mu$ M) for 1 hour at 37°C, washed twice with PBS, lysed with lysis buffer, and the protein obtained was used to measure relative fluorescence at 500 and 530nm excitation and emission, respectively.

#### *Western Blot Analysis*

Twenty-four hours after treatment or exposure to conditioned media, cell lysates were prepared by using NP40 lysis buffer containing protease inhibitors. Protein concentrations were quantitated using bicinchoninic acid (BCA) method. Up to 50  $\mu$ g protein was electrophoresed on 10% polyacrylamide gel and transferred to nitrocellulose membrane (Sigma, St Louis, MO). Membrane was probed with anti-caspase-3 antibody (Cell Signaling Technology, Beverly, MA). The blots were stripped and reprobed with anti- $\beta$ -tubulin to determine equivalent loading. The band intensi-

ties were measured using densitometry and normalized with  $\beta$ -tubulin.

#### *Statistical Analysis*

Experiments for each condition were performed in triplicate and repeated three to five times. Results from each set of experiment were averaged, counted as  $n = 1$  for statistical analysis, and presented as mean  $\pm$  standard deviation. Statistical significance between groups was calculated using analysis of variance followed by Fischer's protected least significant difference test. All values of  $p < 0.05$  were taken as significant.

## **Results**

### *Human Immunodeficiency Virus-1 B- and C-Tat Induce Variable Levels of Monocyte Chemoattractant Protein-1/CC Chemokine Ligand-2 Secretion from Human Astrocytes*

Direct exposure of primary astrocytes to recombinant Tat proteins for 24 hours induced significantly greater levels of CCL2 secretion as compared with the vehicle-treated astrocytes. The Tat-induced CCL2 secretion was not only dose dependent (data not shown), but also the differences between B- or C-Tat and the control cells were statistically significant:  $p < 0.0002$  and  $p < 0.0001$  for B- and C-Tat, respectively (Fig 1A). Interestingly, although C-Tat induced greater levels (1.5-fold from control) of CCL2 compared with the control cells, the induction magnitude was not as high as that of B-Tat (2.5-fold from control), and the difference between the induction of CCL2 levels by Tat proteins was statistically significant ( $p < 0.003$ ). Because we noticed that C-Tat induced CCL2 levels to greater than control cells, we further probed to determine whether both B-Tat- and C-Tat-induced increases in CCL2 production were NF- $\kappa$ B mediated. We pretreated the human astrocytes with an NF- $\kappa$ B inhibitor, pyrrolidine dithiocarbamate, for 60 minutes at 500nM concentration, before B- and C-Tat treatments, and measured the CCL2 production. Interestingly, pyrrolidine dithiocarbamate decreased the CCL2 production in the B-Tat group (from 2.6-fold to a mere 0.85-fold from control), whereas the CCL2 production in the C-Tat group remain unchanged (1.5-fold to 1.6-fold). This indicates that the B-Tat-induced CCL2 production is NF- $\kappa$ B dependent, whereas the C-Tat-induced CCL2 production is perhaps NF- $\kappa$ B independent.

To examine whether intracellular expression of Tat could augment CCL2 secretion from astrocytes and to simulate the in vivo condition where Tat secreted from infected glial cells could activate the astrocytes, we transfected astrocytes with different Tat expression vectors. Wild-type B-Tat (CC) that contains a dicysteine motif at positions 30 and 31, wild-type C-Tat (CS), and isogenic C-Tat mutant vectors (CC and SC) were

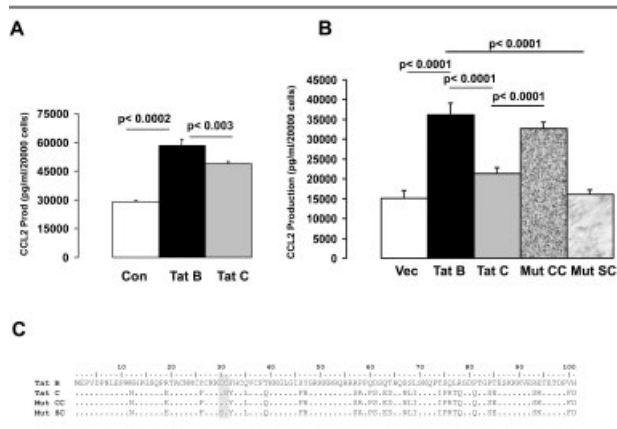


**Fig 1. Human immunodeficiency virus-1 (HIV-1) B- and C-Tat induce differential expression of monocyte chemoattractant protein-1/CC chemokine ligand-2 (MCP-1/CCL2) from human astrocytes. (A) MCP-1/CCL2 production as assayed by enzyme-linked immunosorbent assay from samples of human astrocytes exposed to 100ng/ml concentration of recombinant Tat protein for 24 hours. Note the reduced levels of CCL2 levels in C-Tat group ( $p < 0.003$  vs B-Tat). (B) MCP-1/CCL2 secretion as assayed in conditioned media collected from astrocytes transfected with pcDNA vector, pcDNA B-Tat, pcDNA C-Tat, mutant Tat CC, or mutant SC. Note the significant enhancement in the levels of CCL2 secretion in B-Tat ( $p < 0.0001$  vs vector) and mutant CC groups compared with the C-Tat group ( $p < 0.0001$  vs B-Tat). Differences between B-Tat and mutant SC group, as well as C-Tat and mutant CC group, were also statistically significant ( $p < 0.0001$ ). (C) Amino acid variation between clade B- and C-Tat proteins and in C-Tat mutants. The full-length Tat amino acid sequences of the wild-type B- and C-Tat as well as the two dicysteine isogenic C-Tat variants have been aligned. Dots represent sequence homology. The dicysteine motif is highlighted by gray shading.**

used in the assay. We assayed MCP-1/CCL2 levels in conditioned media collected from astrocytes 24 hours after transfection. Importantly, the CCL2 induction magnitude was statistically significant between the control cells and B-Tat treatment ( $p < 0.0001$ ) but not between the vector control cells and C-Tat treatment, suggesting an attenuated nature of C-Tat (see Fig 1B). Although C-Tat marginally increased levels of CCL2, this difference was not significant. In contrast, the difference in induction levels of CCL2 between B-Tat and C-Tat was statistically significant ( $p < 0.0001$ ), confirming the observations made with the recombinant proteins. Given that subtype B- and C-Tat proteins used in this assay differed from each other at multiple sites (see Fig 1C), the differences seen in CCL2 induction profile could not be ascribed to a particular amino acid variation. Considering the importance of the cysteine-rich domain (CRD) for cytokine induction properties, we included two isogenic C-Tat variants in CCL2 induction studies. One of the variants contained

cysteine at positions 30 and 31 (CC) compared with wild-type C-Tat that contained a cysteine and a serine (CS) thus homologous to wild-type B-Tat. The other variant contains a serine and a cysteine (SC) at these positions and is expected to be defective for several biological functions including the transactivation. Remarkably, C-Tat (CC) restored the induction levels of CCL2 from astrocytes almost to the same extent as the wild-type B-Tat. The C-Tat (SC) failed to do so and behaved more like the wild-type C-Tat (see Fig 1B).

This observation is important because it suggests that the reduction in CCL2 levels with C-Tat (CS) is dependent on the presence of CS motif at position 31 (see Fig 1B).

### Human Immunodeficiency Virus-1 B- and C-Tat Induce Different Levels of Neuronal Apoptosis

Treatment of primary neuronal cultures with nanogram per milliliter concentration of Tat proteins induced accelerated levels of neuronal death within 24 hours in a dose-dependent manner as assessed by two different methods, the TUNEL assay and the MTT assay. Whereas the TUNEL assay works based on labeling of the damaged DNA portion of the apoptotic cells, the MTT assay works based on formazan crystal formation by live cells. Data obtained with B-Tat are consistent with previous observations made by other investigators.<sup>31–33</sup>

In the TUNEL assay, we observed approximately 50% apoptotic cells within 24 hours, when the cultures of human neurons were exposed to B-Tat protein at a concentration of 100ng/ml. The Tat-induced neuronal apoptosis was not only dose-dependent but also statistically significant as compared with vehicle control neurons that were treated under similar conditions with 1X PBS (Fig 2A). In contrast, C-Tat protein failed to induce high-level apoptosis. The difference between the levels of apoptosis induced in neurons by B- and C-Tat proteins was statistically different ( $p < 0.01$ ), which is intriguing (see Fig 2A).

We then evaluated cell apoptosis using TUNEL assay in neurons that were exposed to conditioned media collected from astrocytes that were transfected with various Tat expression vectors, that is, pcDNA alone, pcDNA B-Tat, pcDNA C-Tat, and mutant C-Tat (CC and SC), to simulate the indirect cell death pathway. As was noticed with the recombinant proteins, neuron apoptosis was highest when exposed to B-Tat conditioned media ( $p < 0.0016$ ), but not C-Tat conditioned media, and the difference between the two Tat vectors was significant ( $p < 0.01$ ). This trend was, however, reversed with C-Tat (CC) conditioned media where neuronal apoptosis was found to be at the same levels as that of wild-type B-Tat (up to 60% cell death). C-Tat (SC) caused cell death barely above the vector treatment, and this phenotype is similar to that

of the wild-type C-Tat (see Fig 2B). These data ascertained the pathological significance of the dicysteine motif in Tat for neuropathogenesis.

To confirm our observations of TUNEL assays, we performed a widely accepted cell viability assay, the MTT assay in a 96-well format where the exposure of neurons to Tat protein and astrocyte conditioned media were done exactly as described in TUNEL assay. Similar to TUNEL assay, we found that cell death was greatest in neurons treated either with B-Tat protein (see Fig 2C) or with conditioned media (see Fig 2D) from B-Tat transfected astrocytes, noticed as significant decrease in cell viability. As seen in TUNEL assay, MTT assay of human neurons also showed that cell death was significantly lower in neurons that were exposed to C-Tat protein ( $p < 0.0001$ ) or in groups that were treated with conditioned media from C-Tat transfected astrocytes ( $p < 0.0003$ ), compared with respective B-Tat groups. However, conditioned media from mutant C-Tat (CC) transfected astrocytes exhibited cell death quite similar to those noticed with B-Tat groups (see Fig 2D). The mutant SC group showed negligible cell death. The differences between the relevant test groups were statistically significant.

We also studied the morphology of human primary neuronal cultures that were exposed to conditioned media from astrocytes transfected with various expression vectors for 24 hours. The morphology of cells clearly was indicative of the results obtained in various parameters studied (data not shown). Neuronal damage

was significantly low in C-Tat and mutant SC groups, and maximum in the B-Tat groups.

### B- and C-Tat Induce Different Levels of Oxidative Stress in Neurons

To further investigate the pathways that may be involved in the B-Tat- and C-Tat-mediated neuronal damage, we measured the ROS production in neurons exposed either to vehicle, B-Tat, or C-Tat protein at 100ng/ml concentration for 24 hours. ROS assays were also performed on neurons exposed to conditioned media from pcDNA vector, pcDNA B-Tat, pcDNA C-Tat, or pcDNA mutants C-Tat (CC and SC). We observed a substantial augmentation in ROS generation after B-Tat exposure ( $p < 0.003$ ). The ROS levels in the C-Tat protein-treated group, however, were sig-

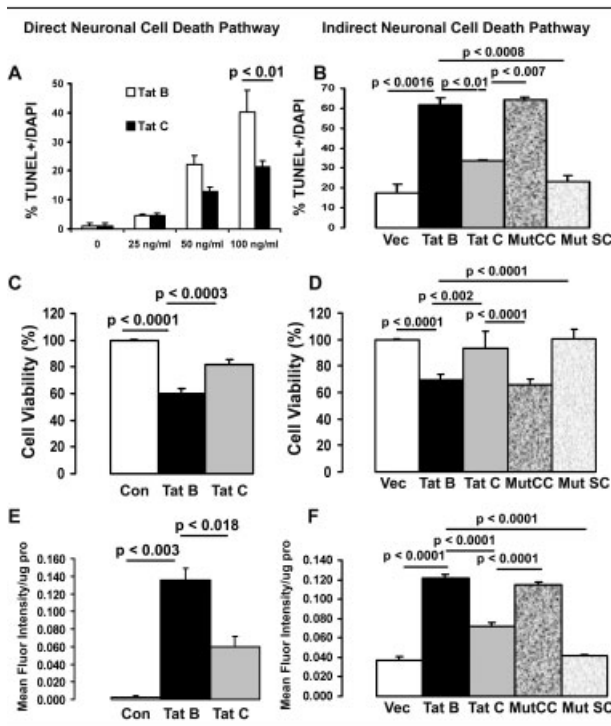


Fig 2. Human primary neurons undergo damage by direct and indirect cell death pathway after exposure to human immunodeficiency virus-1 (HIV-1) Tat from clades B and C. (A) Quantitative assessment of human neurons undergoing apoptosis after 24-hour exposure to HIV-1 B- and C-Tat protein represented as percentage of terminal deoxynucleotidyltransferase-mediated dUTP nick end labeling (TUNEL)-stained nuclei/4',6-diamidino-2-phenylindole (DAPI)-positive nuclei ( $n = 3$ ). (B) Quantitative assessment of TUNEL-positive human neurons undergoing apoptosis after exposure to conditioned media from astrocytes transfected with the parental vector (Vec) and different Tat-expressing vectors as shown. Note the remarkable levels of attenuation in the C-Tat group ( $p < 0.01$  vs B-Tat;  $n = 5$ ) and reversal of attenuation of apoptosis in the mutant CC group ( $p < 0.007$  vs C-Tat). (C) Cell viability of human primary neuronal cultures treated with HIV-1 Tat protein from clade B or C as assessed by the MTT (3-[4,5-dimethylthiazol-2-yl]-2,5-diphenyl-tetrazolium bromide) assay, depicting direct cell death pathway. Neurons in C-Tat group show larger number of viable cells compared with the B-Tat group ( $p < 0.0001$ ;  $n = 6$ ). (D) Cell viability assay of human neurons after exposure to conditioned media from astrocytes transfected with Tat-expressing vectors, depicting indirect cell death pathway. Note the reduced magnitude of cell viability in the B-Tat ( $p < 0.0001$ ) and mutant CC groups, and negligible damage of neurons in the C-Tat and mutant Tat SC groups ( $n = 5$ ). Data represent mean  $\pm$  standard deviation. (E, F) HIV-1 B- and C-Tat induce different levels of oxidative stress in human primary neurons. Human neurons undergoing varied levels of oxidative stress as measured by the levels of the reactive oxygen species (ROS) using 7'-dichlorodihydrofluorescein diacetate (DCFDA) probe represented by mean fluorescence intensity per microgram protein. (E) Levels of reactive oxygen species generated from human neurons treated with B- and C-Tat protein, depicting direct cell death pathway. (F) Levels of ROS generated from human neurons after exposure to astrocyte conditioned media, depicting indirect cell death pathway. Note that ROS levels in the B-Tat and mutant CC groups are at a similar range, indicating importance of the dicysteine motif for oxidative stress. Data represent mean  $\pm$  standard deviation of three independent experiments.

nificantly lower ( $p < 0.018$ ) in comparison with the B-Tat group (see Fig 2E), indicating that C-Tat mediates a weak oxidative stress on neurons. In the indirect neurotoxicity model, culture of human neurons with conditioned media from B-Tat transfected astrocytes showed significantly enhanced ROS levels ( $p < 0.0001$ ); however, in the C-Tat group, the ROS generation was comparable with the vector control group. Neurons cultured with conditioned media from astrocytes transfected with mutant C-Tat (CC) exhibited ROS generation in levels quite similar to those seen with B-Tat expression vectors (see Fig 2F).

#### Human Immunodeficiency Virus-1 C-Tat Induces Weaker Mitochondrial Membrane Depolarization in Neurons

Differential neuronal death patterns seen with HIV-1 B-Tat and C-Tat proteins, as well as with astrocyte conditioned media, prompted us to examine the neuronal mitochondrial membrane depolarization. JC-1 is a fluorescent lipophilic cationic dye that is sequestered in mitochondria in proportion to the electrical potential differential that normally exists across the inner mitochondrial membrane.<sup>34</sup> Recently, several investigators used this agent to assess the status of mitochondrial membrane potential in cultured neurons undergoing neurotoxicity.<sup>35,36</sup> To assess the mitochondrial membrane potential, we added JC-1 dye to human neuronal cultures after they were exposed to Tat proteins or conditioned media from Tat transfected astrocytes. We found that exposure to B-Tat resulted in significant depolarization of the mitochondrial membrane as seen by the substantial decrease in the red/green ratio, clearly indicating that the B-Tat treatments induce cell death by mitochondrial membrane depolarization and possibly resulting in release of cytochrome *c* from mitochondria. Treatment of neuronal cultures with conditioned media from C-Tat transfected astrocytes, however, resulted in little or no depolarization of the mitochondrial membrane as seen with JC-1 dye treatment (Fig 3A). We obtained similar results with Tat protein or the direct cell death pathway (data not shown).

Identical to our observations with other parameters used in this study, introduction of conditioned media from astrocytes treated with mutant C-Tat (CC) resulted in the depolarization of neurons, similar to levels that were observed with B-Tat groups (see Fig 3A).

#### Human Immunodeficiency Virus-1 B- and C-Tat Exhibit Variations in Cleaved Caspase-3 Expression in Human Primary Neurons

To delineate the pathway of apoptosis induced by Tat, we performed Western blotting of neuronal cell extract for caspase-3. Neurons were exposed to Tat-conditioned astrocyte media before Western blotting. A

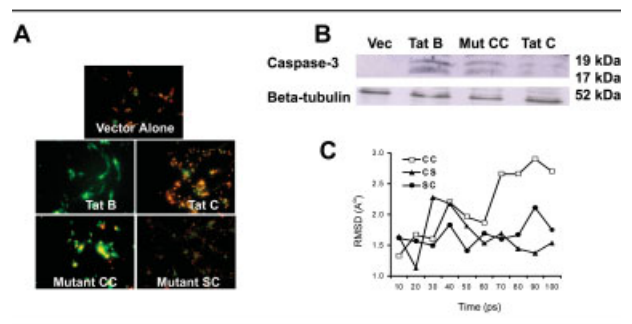


**Fig 3. Modulation of mitochondrial membrane potential and caspase activation in human neurons is clade specific.** (A) Composite depicts effect of Tat on mitochondrial membrane potential in human neurons as assessed by using the JC-1 probe. Note the formation of JC-1 green aggregates after exposure of human neurons to conditioned media from Tat-transfected astrocytes. The intense green aggregates in the B-Tat and mutant C-Tat CC groups indicate considerable depolarization of mitochondrial membranes. (B) Western blot showing the expression of cleaved caspase-3 in protein samples from human neurons cultured with the astrocyte conditioned media. Note that human neurons treated with conditioned media from HIV-1 C-Tat transfected astrocytes express low levels of cleaved caspase-3 protein (last lane) compared with others. Data are representative of results obtained from two independent experiments. Densitometric measurements were performed on individual immunoblots for each antibody tested. Caspase-3 expression is significantly low from the C-Tat group as compared with B-Tat ( $p < 0.05$ ) (data not shown here). (C) Graph depicts the molecular simulation dynamics of the cysteine-rich domain of subtype C-Tat and its variants. Ten picoseconds (ps) of equilibration at 300 Kelvin were followed by 100 ps of molecular dynamics (MD) simulation, and root mean square displacement (RMSD) was measured. RMSD of the wild-type CS-Tat (triangles) for 10 representative MD-derived structures was found to be a maximum of 2.3Å. The root mean square displacement value for CC-Tat (squares) 2.9Å and SC-Tat (circles) 2.11Å was significantly greater than CS-Tat, indicating higher order of flexibility.

cleaved caspase-3 protein was visible quite distinctly in B-Tat group, but not in C-Tat group. As observed in other parameters studied, cultures of neuron with media from mutant CC transfected astrocytes resulted in cleaved caspase-3 expression quite similar to those of B-Tat group, signifying the importance of dicysteine motif for Tat neuropathogenesis (see Fig 3B). Similar results were obtained with Tat protein treatment (data not shown). To confirm that the Tat-induced neuronal damage is caspase dependent, we used a known caspase inhibitor Z-VAD FMK (carboxymethyl-valyl-alanyl-aspartyl-[O-methyl]-fluoromethylketone) at a concentration of 50μM. We observed that neuronal apoptosis was considerably reduced after pretreatment with the caspase inhibitor, confirming that Tat neurotoxicity is via the caspase pathway.

These data collectively demonstrate that clade iden-

tity of Tat has significant impact on neuronal pathogenesis. Tat from two important clades of HIV-1 induced apoptosis in human neurons to variable degrees with C-Tat invariably being inferior to B-Tat in all the assays used here. The data on the mechanism of neuron apoptosis suggested that B- and C-Tat caused differential degrees of perturbation at the level of the mitochondrial membrane and oxidative stress that ultimately triggered the caspase cascade pathway, activation of caspase-3 that finally pushed the neuron into apoptosis.

## Discussion

Data presented here point to significant clade-specific differences in HIV-1 Tat-induced cell death of human neurons. Unlike HIV-1 B-Tat, the neuronal damage by HIV-1 C-Tat was of a considerable low intensity, and there were distinct differences in the levels of up-regulation at several steps of intrinsic apoptotic pathway. Furthermore, clade-specific differences in Tat-induced neuronal apoptosis were observed in both direct and indirect modes of neuronal damage after exposure of human neurons to Tat. Importantly, data presented here highlight the pathogenic significance of the dicysteine motif in Tat. A natural variation in C-Tat in the dicysteine motif possibly underlies the differential neuronal damage observed by Tat originated from clades B and C. This article demonstrates remarkable clade-specific differences in HIV-1 B- and C-Tat proteins causing apoptosis in human neurons.

Neuronal apoptosis has been documented through pathological examination of brains from HIV-1-infected and demented patients from HIV-1 clade B-prevalent countries such as the Americas and Europe, where incidence of HIV-1-associated neurological manifestations is reportedly greater. The neurobiology of HIV-1 clade B viruses is comparatively well studied and understood. Unfortunately, studies on postmortem brains from HIV-1 C-infected individuals are lacking because autopsies on AIDS patients are rarely performed in developing countries, including India. Furthermore, as the animal models for NeuroAIDS have not been successful, use of *in vitro* cell culture system of human brain cells is mandatory. We used primary human neuronal cultures with minimal glial cell contamination to evaluate the neurotoxic potential of viral protein Tat derived from two important clades that account for the majority of global viral infections.

To understand the possible differences between these important clades of HIV-1, we chose HIV-1 Tat protein based on its known neurotoxic properties and its significance for HIV-1-associated neurological deficits in infected individuals. Given that subtype/clade C-Tat differs from other viral subtypes in lacking a dicysteine motif, we elected to use wild-type B- and C-Tat and

dicysteine variant forms of C-Tat to evaluate the neurotoxic epitope of Tat rather than using the overlapping synthetic peptides of the Tat protein. In carefully designed experiments, we examined both direct and indirect neuronal damage pathways that are typically known to occur in HIV-1-associated dementia.<sup>8,37</sup> For direct damage pathway, we treated human neurons with clade-specific HIV-1 Tat protein. To evaluate the indirect damage pathway and in an attempt to simulate pathological conditions that may be arising after infection of HIV-1 in human astrocytes, we transfected human astrocyte cultures with Tat-expression vectors. Transfected astrocytes expressed and released Tat into the culture media as they do in the infected human brain.

We confirmed secretion of Tat from transfected astrocytes with the help of Tat polyclonal antibody that were raised by us in rabbit, before advancing with experiments on human neuronal cultures (data not shown). Incubation of conditioned media with polyclonal Tat antibody significantly reduced the number of TUNEL-positive cells, further confirming that the neurotoxic effects of conditioned media are perhaps due to presence of Tat that would be secreted from astrocytes transfected with various Tat-expressing vectors. We are aware that astrocytes cannot support a productive viral infection; however, a previous study demonstrated synthesis and extracellular secretion of viral proteins when human astrocytes were transfected with pNL4-3 DNA vector.<sup>38</sup> Considering the importance of the astrocytes for neuron survival and functioning in the natural context and the role astrocytes are believed to play in Tat-induced excitotoxic injury to the neurons in viral infection, we used an astrocyte/neuron model in this study.

Our observation that Tat-induced damage to human neurons is mediated via apoptosis caused by alterations in mitochondrial membrane potential, oxidative stress, and ultimately in the activation of caspase-3 is consistent with studies reported previously. Our study provides convincing evidence that there is a differential degree of neuronal damage induced by B- and C-Tat, and that could be ascribed to the variation of a single amino acid at position 31 in the neurotoxic region of the Tat protein. Our observations are also in line with the recent reports that studied clade-specific differences in HIV-1 B- and C-Tat protein for production of inflammatory cytokines interleukin-6 and tumor necrosis factor- $\alpha$  in peripheral blood monocytes, as well as compromised monocyte chemotactic function of C-Tat.<sup>25,28</sup> Mitochondria play a crucial role in apoptosis. Disruption of mitochondrial transmembrane potential is a critical early event that triggers the process of cell death through a series of events including uncoupling of oxidative phosphorylation, generation of ROS, release of cytochrome *c* from the mitochondria

into the cytosol, and activation of the caspase cascade that finally ends up in cellular apoptosis. We studied alterations in mitochondrial membrane potential of human neurons by using the JC-1 dye and dissected several other critical steps in the pathway that indicate there are clear differences in the effect of B- and C-Tat on mitochondrial membrane potential and ultimately in caspase-3 activation and neuronal apoptosis. Similar experiments with human astrocytes demonstrated that Tat concentrations (50 and 100ng/ml) that were toxic to human neurons were unable to induce noticeable apoptosis in astrocytes. The JC-1 staining of human astrocytes with and without Tat did not elicit any alterations, indicating that human astrocytes are possibly unaffected at these concentrations. Our observations also suggest that differences of neurotoxicity between clades C and B may be used as a molecular tool to dissect pathways of neuronal apoptosis.

It has been hypothesized that clade-specific differences of HIV-1 subtype C-Tat underlie the reported low incidence of HIV-1-associated dementia in India; however, a direct correlation between reduced neurotoxic potential of C-Tat and HIV-1-associated neurological deficits is lacking. We therefore investigated whether clade-specific differences in B- and C-Tat proteins could differentially modulate neuronal apoptosis. With carefully designed experiments and appropriate controls, we thoroughly investigated the neurotoxic potential of B- and C-Tat. Using different models of neuronal cell damage, we evaluated and confirmed attenuated neuropathogenic nature of C-Tat in comparison with B-Tat. Use of isogenic variants of C-Tat not only ascertained the reduced neurotoxic potential of C-Tat for human neurons but also confirmed the neuropathological significance of the dicysteine motif in Tat. This variation at position 31 of C-Tat has previously been shown to be critical for the induction of inflammatory cytokine production from human peripheral blood mononuclear cells.<sup>25</sup> Recently, the importance of point mutations in the coding region of prion proteins at position 129 in neuropathogenesis in prion disease has also been reported.<sup>39,40</sup> Data on Tat structure and its domains are scarce for technical reasons. First, Tat, like several other transactivation factors, is highly flexible and lacks well-structured three-dimensional folds.<sup>41,42</sup> Only low-resolution nuclear magnetic resonance structure, but not X-ray crystal structure, of Tat is available.<sup>43,44</sup> Second, most of the reports of Tat structure derived from subtype B viral protein.<sup>42</sup> Only a limited number of studies used Tat of other viral subtypes. The variation within the CRD of Tat is a characteristic feature of subtype C-Tat, and virtually no studies determined the molecular structure of Tat from subtype C. As a result, the information on the structural differences within subtype C-Tat at the gross level

and at individual domain level is unknown. Such studies are yet to commence.

Circular dichroism analyses of Tat derived from subtypes B and D in aqueous solutions identified primarily random coil structures and/or  $\alpha$ -turns. Importantly, minor structural variations in Tat are implied to influence the pathogenic properties of the viral protein.<sup>45</sup> Using circular dichroism analysis, Ranga's group<sup>25</sup> reported important differences between B- and C-Tat proteins. They alluded to a possible higher ordered and less flexible structure in subtype C-Tat protein compared with B-Tat.<sup>28</sup> Ranga's group identified natural variations within the CRD of subtype C-Tat<sup>25</sup> and offered important clues as per the structural consequences.<sup>28</sup> Apart from this single study, no information is available on the possible structural differences of Tat proteins, their domains, and a possible influence of such differences on the biological functions of Tat.

To fill in this gap, we performed molecular dynamics simulation to explore the conformational variation existing within the CRD domain of Tat (residues 15–37). Molecular dynamics simulations are used to investigate dynamics and intramolecular interactions of proteins in aqueous solution, and such analyses have been applied to HIV-1 Tat previously.<sup>46,47</sup> The molecular dynamics simulation examined only the 22 residues of the CRD region of Tat, whereas the rest of the protein was constrained. Subtype C wild-type Tat (CS) and its two cysteine variants (CC and SC) were included in the analysis. Root mean square displacement of the wild-type CS-Tat for 10 representative molecular dynamics-derived structures was found to be a maximum of 2.3Å (see Fig 3C). The root mean square displacement value for CC-Tat (2.9Å) and SC-Tat (2.11Å) was significantly greater than CS-Tat. An increase in the root mean square displacement value is indicative of higher order of flexibility. These data suggest that Tat CRD containing a dicysteine motif (subtype B-like) is likely to contain more structural flexibility than its isogenic form containing a CS (subtype C-like) variation ascertaining the prediction made by some of us previously.<sup>28</sup> We did not include subtype B-Tat in this analysis because the CRD and other domains of Tat contain significant levels of intrasubtype and intersubtype variations. It is nevertheless possible to extrapolate these results to the CRD of subtype B-Tat. The molecular dynamic simulation corroborates the above premise that B-Tat is relatively more flexible than C-Tat. This relative higher order of flexibility of B-Tat, in turn, might explain its higher biological activity described in this article and previously.<sup>28</sup> High-resolution structures of nuclear magnetic resonance are needed to understand the differences between C-Tat and Tat proteins of other subtypes, but this is beyond the scope of this study.

Interestingly, subtype C-Tat protein is also naturally

devoid of the arginine-glycine-aspartic acid (RGD) motif in exon 2, which is necessary for Tat to attach to the integrin receptors  $\alpha 5\beta 1$  and  $\alpha v\beta 3$  on the cell surface.<sup>48,49</sup> Tat binds the target cells in a dose-dependent manner using the RGD motif, and Tat mutants lacking the RGD motif fail to mediate efficient cell adhesion.<sup>48</sup> Absence of this motif may adversely affect cell attachment of C-Tat and the subsequent internalization. We are currently comparing additional Tat clones from subtype B and C primary clinical isolates to confirm this observation.

Although data presented here using recombinant Tat proteins and Tat-expression vectors substantiate clade-specific manifestation on viral neuropathogenesis, these observations must be ascertained using infectious viruses. Some of these experiments are currently in progress in our laboratory. Detailed studies with post-mortem human brain samples from HIV-1 patients from clade B and C endemic areas are warranted to further validate these findings.

In conclusion, using recombinant Tat proteins, Tat expression vectors, and isogenic subtype C-Tat variants, we demonstrated clade-specific differences in neuropathogenic properties of Tat. Clade C-Tat protein demonstrated highly attenuated phenotype and caused only mild levels of neuron apoptosis compared with clade B-Tat. We believe that this study is an important milestone toward understanding clade-specific neurotoxic properties of Tat for human neurons and a significant advancement in our limited understanding of neuropathobiology of HIV-1 clades B and C.

---

This study was supported by the Department of Biotechnology, Ministry of Science and Technology, India (BT/PR6838/Med/14/881/2005, P.S.), Senior Research Fellowship from National Brain Research Centre, India (M.M.), Department of Biotechnology, Government of India (BT/PR5355/Med/14/623/2004, U.R.), and Indian Council of Medical Research, Government of India (Immuno/18/11/19/2002-ECD-I, U.R.).

We acknowledge help from S. Reddy in standardizing a few assays used in the study and technical assistance from D. Lal Meena during the study. We also acknowledge Prof V. Ravindranath and Prof P. N. Tandon for their constant support and encouragement to make this work possible, and Dr A. Basu for valuable discussions. We are grateful to Dr D. Sethi for his help with the Tat structure analysis in the study.

---

## References

1. Clements JE, Zink MC. Molecular biology and pathogenesis of animal lentivirus infections. *Clin Microbiol Rev* 1996;9:100–117.
2. McArthur JC. Neurologic manifestations of AIDS. *Medicine* 1987;66:407–437.
3. Eugenin EA, Osiecki K, Lopez L, et al. CCL2/monocyte chemoattractant protein-1 mediates enhanced transmigration of human immunodeficiency virus (HIV)-infected leukocytes across the blood-brain barrier: a potential mechanism of HIV-CNS invasion and NeuroAIDS. *J Neurosci* 2006;26:1098–1106.

4. Conant K, Garzino-Demo A, Nath A, et al. Induction of monocyte chemoattractant protein-1 in HIV-1 Tat-stimulated astrocytes and elevation in AIDS dementia. *Proc Natl Acad Sci U S A* 1998;95:3117–3121.
5. Kolb SA, Sporer B, Lahrtz F, et al. Identification of a T cell chemotactic factor in the cerebrospinal fluid of HIV-1-infected individuals as interferon-gamma inducible protein 10. *J Neuroimmunol* 1999;93:172–181.
6. van Marle G, Henry S, Todoruk T, et al. Human immunodeficiency virus type 1 Nef protein mediates neural cell death: a neurotoxic role for IP-10. *Virology* 2004;329:302–318.
7. Kelder W, McArthur JC, Nance-Sproson T, et al. Beta-chemokines MCP-1 and RANTES are selectively increased in cerebrospinal fluid of patients with human immunodeficiency virus-associated dementia. *Ann Neurol* 1998;44:831–835.
8. Gonzalez-Scarano F, Martin-Garcia J. The neuropathogenesis of AIDS. *Nat Rev* 2005;5:69–81.
9. Weis S, Haug H, Budka H. Neuronal damage in the cerebral cortex of AIDS brains: a morphometric study. *Acta Neuropathol (Berl)* 1993;85:185–189.
10. Nath A. Human immunodeficiency virus (HIV) proteins in neuropathogenesis of HIV dementia. *J Infect Dis* 2002;186(suppl 2):S193–S198.
11. Kruman, II, Nath A, Mattson MP. HIV-1 protein Tat induces apoptosis of hippocampal neurons by a mechanism involving caspase activation, calcium overload, and oxidative stress. *Exp Neurol* 1998;154:276–288.
12. Aksenov MY, Hasselrot U, Bansal AK, et al. Oxidative damage induced by the injection of HIV-1 Tat protein in the rat striatum. *Neurosci Lett* 2001;305:5–8.
13. Aksenov MY, Hasselrot U, Wu G, et al. Temporal relationships between HIV-1 Tat-induced neuronal degeneration, OX-42 immunoreactivity, reactive astrocytosis, and protein oxidation in the rat striatum. *Brain Res* 2003;987:1–9.
14. Korber BT, Allen EE, Farmer AD, Myers GL. Heterogeneity of HIV-1 and HIV-2. *Aids* 1995;9(suppl A):S5–S18.
15. Blackard JT, Renjifo B, Fawzi W, et al. HIV-1 LTR subtype and perinatal transmission. *Virology* 2001;287:261–265.
16. Jeeninga RE, Hoogenkamp M, Armand-Ugon M, et al. Functional differences between the long terminal repeat transcriptional promoters of human immunodeficiency virus type 1 subtypes A through G. *J Virol* 2000;74:3740–3751.
17. Roof P, Ricci M, Genin P, et al. Differential regulation of HIV-1 clade-specific B, C, and E long terminal repeats by NF-kappaB and the Tat transactivator. *Virology* 2002;296:77–83.
18. Ndung'u T, Sepako E, McLane MF, et al. HIV-1 subtype C in vitro growth and coreceptor utilization. *Virology* 2006;347:247–260.
19. Siddappa NB, Dash PK, Mahadevan A, et al. Identification of subtype C human immunodeficiency virus type 1 by subtype-specific PCR and its use in the characterization of viruses circulating in the southern parts of India. *J Clin Microbiol* 2004;42:2742–2751.
20. Esparza J, Bhamarapravati N. Accelerating the development and future availability of HIV-1 vaccines: why, when, where, and how? *Lancet* 2000;355:2061–2066.
21. McCutchan FE. Understanding the genetic diversity of HIV-1. *AIDS* 2000;14(suppl 3):S31–S44.
22. Shankar SK, Mahadevan A, Satishchandra P, et al. Neuropathology of HIV/AIDS with an overview of the Indian scene. *Indian J Med Res* 2005;121:468–488.
23. Satishchandra P, Nalini A, Gourie-Devi M, et al. Profile of neurologic disorders associated with HIV/AIDS from Bangalore, south India (1989-96). *Indian J Med Res* 2000;111:14–23.

24. Hu DJ, Buve A, Baggs J, et al. What role does HIV-1 subtype play in transmission and pathogenesis? An epidemiological perspective. *AIDS* 1999;13:873–881.
25. Ranga U, Shankarappa R, Siddappa NB, et al. Tat protein of human immunodeficiency virus type 1 subtype C strains is a defective chemokine. *J Virol* 2004;78:2586–2590.
26. Nath A, Psooy K, Martin C, et al. Identification of a human immunodeficiency virus type 1 Tat epitope that is neuroexcitatory and neurotoxic. *J Virol* 1996;70:1475–1480.
27. Messam CA, Hou J, Gronostajski RM, Major EO. Lineage pathway of human brain progenitor cells identified by JC virus susceptibility. *Ann Neurol* 2003;53:636–646.
28. Siddappa NB, Venkatramanan M, Venkatesh P, et al. Transactivation and signaling functions of Tat are not correlated: biological and immunological characterization of HIV-1 subtype-C Tat protein. *Retrovirology* 2006;3:53.
29. Seth P, Diaz F, Tao-Cheng JH, Major EO. JC virus induces nonapoptotic cell death of human central nervous system progenitor cell-derived astrocytes. *J Virol* 2004;78:4884–4891.
30. Schreck R, Baeuerle PA. Assessing oxygen radicals as mediators in activation of inducible eukaryotic transcription factor NF-kappa B. *Methods Enzymol* 1994;234:151–163.
31. Singh IN, Goody RJ, Dean C, et al. Apoptotic death of striatal neurons induced by human immunodeficiency virus-1 Tat and gp120: differential involvement of caspase-3 and endonuclease G. *J Neurovirol* 2004;10:141–151.
32. Bonavia R, Bajetto A, Barbero S, et al. HIV-1 Tat causes apoptotic death and calcium homeostasis alterations in rat neurons. *Biochem Biophys Res Commun* 2001;288:301–308.
33. New DR, Ma M, Epstein LG, et al. Human immunodeficiency virus type 1 Tat protein induces death by apoptosis in primary human neuron cultures. *J Neurovirol* 1997;3:168–173.
34. Cossarizza A, Baccarani-Contri M, Kalashnikova G, Franceschi C. A new method for the cytofluorimetric analysis of mitochondrial membrane potential using the J-aggregate forming lipophilic cation 5,5',6,6'-tetrachloro-1,1',3,3'-tetraethylbenzimidazolcarbocyanine iodide (JC-1). *Biochem Biophys Res Commun* 1993;197:40–45.
35. Keswani SC, Polley M, Pardo CA, et al. Schwann cell chemokine receptors mediate HIV-1 gp120 toxicity to sensory neurons. *Ann Neurol* 2003;54:287–296.
36. Gartlon J, Kinsner A, Bal-Price A, et al. Evaluation of a proposed in vitro test strategy using neuronal and non-neuronal cell systems for detecting neurotoxicity. *Toxicol In Vitro* 2006;20:1569–1581.
37. King JE, Eugenin EA, Buckner CM, Berman JW. HIV tat and neurotoxicity. *Microbes Infect* 2006;8:1347–1357.
38. Tornatore C, Nath A, Amemiya K, Major EO. Persistent human immunodeficiency virus type 1 infection in human fetal glial cells reactivated by T-cell factor(s) or by the cytokines tumor necrosis factor alpha and interleukin-1 beta. *J Virol* 1991;65:6094–6100.
39. Asante EA, Linehan JM, Gowland I, et al. Dissociation of pathological and molecular phenotype of variant Creutzfeldt-Jakob disease in transgenic human prion protein 129 heterozygous mice. *Proc Natl Acad Sci U S A* 2006;103:10759–10764.
40. Yin S, Pham N, Yu S, et al. Human prion proteins with pathogenic mutations share common conformational changes resulting in enhanced binding to glycosaminoglycans. *Proc Natl Acad Sci U S A* 2007;104:7546–7551.
41. Shojania S, O'Neil JD. HIV-1 Tat is a natively unfolded protein: the solution conformation and dynamics of reduced HIV-1 Tat-(1-72) by NMR spectroscopy. *J Biol Chem* 2006;281:8347–8356.
42. Bayer P, Kraft M, Ejchart A, et al. Structural studies of HIV-1 Tat protein. *J Mol Biol* 1995;247:529–535.
43. Gregoire C, Peloponese JM Jr, Esquieu D, et al. Homonuclear (1)H-NMR assignment and structural characterization of human immunodeficiency virus type 1 Tat Mal protein. *Biopolymers* 2001;62:324–335.
44. Peloponese JM Jr, Gregoire C, Opi S, et al. 1H–13C nuclear magnetic resonance assignment and structural characterization of HIV-1 Tat protein. *C R Acad Sci III* 2000;323:883–894.
45. Peloponese JM Jr, Collette Y, Gregoire C, et al. Full peptide synthesis, purification, and characterization of six Tat variants. Differences observed between HIV-1 isolates from Africa and other continents. *J Biol Chem* 1999;274:11473–11478.
46. Pantano S, Carloni P. Comparative analysis of HIV-1 Tat variants. *Proteins* 2005;58:638–643.
47. Pantano S, Tyagi M, Giacca M, Carloni P. Molecular dynamics simulations on HIV-1 Tat. *Eur Biophys J* 2004;33:344–351.
48. Brake DA, Debouck C, Biesecker G. Identification of an Arg-Gly-Asp (RGD) cell adhesion site in human immunodeficiency virus type 1 transactivation protein, tat. *J Cell Biol* 1990;111:1275–1281.
49. Barillari G, Gendelman R, Gallo RC, Ensoli B. The Tat protein of human immunodeficiency virus type 1, a growth factor for AIDS Kaposi sarcoma and cytokine-activated vascular cells, induces adhesion of the same cell types by using integrin receptors recognizing the RGD amino acid sequence. *Proc Natl Acad Sci U S A* 1993;90:7941–7945.